the organizing element which promoted complex formation was the polymer, to which pyrochlorophyll was bound by ligation and DTNB by counterion attraction. In the present case, the organizing element is evidently the cationic micelle.

Chl and its relatives have been examined in almost every conceivable kind of model system in efforts to imitate photosynthesis. To our recollection, however, this is the first report of its presence in cationic inverted micelles. Chl has been reported in anionic inverted micelles of aerosol OT[18] though these may have been more in the nature of microemulsions, with a clearly defined internal aqueous phase. Inverted micelles have been promoted as models of the interiors of proteins or lipoproteins, where numerous biological reactions, including the primary processes of photosynthesis, take place.[11,19] It may be that systems such as the present one will be useful in the investigation of biomimetic models.

Acknowledgment. This work was supported in part by the Division of Chemical Sciences, Office of Basic Energy Sciences, U.S. Department of Energy, under Grant No. DE-FG02-86ER13620 to G.R.S. and by Grant No. DE-FG02-87ER13791 to D. Gust and T. A. Moore. The Arizona State University Center for the Study of Early Events in Photosynthesis is funded by the U.S. Department of Energy Grant DE-FG02-88ER13969 as part of the USDA/DOE/NSF Plant Science Center Program.

Registry No. Chl, 479-61-8; DPI, 3026-66-2; DTNP, 2127-10-8; DTNB·2TMA, 124687-71-4.

(18) Pileni, M. P.; Lerebours, B.; Brochette, P.; Chevalier, Y. *J. Photochem.* **1985**, *28*, 273.

(19) Vos, K.; Laane, C.; Visser, A. J. W. G. *Photochem. Photobiol.* **1987**, *45*, 863.

Photovoltaic Effect in Symmetrical Cells of a Liquid Crystal Porphyrin

Brian A. Gregg, Marye Anne Fox,* and Allen J. Bard*

Department of Chemistry, University of Texas at Austin, Austin, Texas 78712 *(Received: May 23, 1989; In Final Form: August 16, 1989)*

An unusual photovoltaic effect has been observed in symmetrical cells consisting of indium–tin oxide (ITO) electrodes and a liquid crystal porphyrin (LCP, zinc octakis(β-octyloxyethyl)porphyrin). The illuminated electrode acts as a photoanode; the direction of current flow reverses upon reversal of the direction of illumination. Stable photocurrents of up to ca. 0.4 mA/cm^2 have been measured under illumination with a 150-W Xe lamp (intensity ca. 150 mW/cm^2). The photocurrent increases linearly with incident light intensity (I_0) at all wavelengths up to $I_0 > 10^{15}$ photons s^{-1} cm^{-2}. This photovoltaic effect is interpreted as resulting from exciton dissociation at the illuminated electrode leading to the preferential photoinjection of electrons into the ITO electrode and holes into the porphyrin. This appears to be the first unambiguous example of a photovoltaic cell controlled entirely by interfacial kinetics. The predominance of the photoinjection process in these capillary-filled liquid crystal (solid-phase) films, and its relative absence in similar cells containing evaporated films of porphyrins and phthalocyanines, is attributed to the single-crystal-like character of the LCP films. The wavelength dependence of the photocurrent (action spectrum) is a function of the cell thickness, correlating with the absorption spectrum for thin cells, while it is inversely correlated for thicker cells. This is attributed to an effective cell resistance that is determined by the number and spatial distribution of carriers photogenerated in the bulk LCP. An approximate mathematical model of these two processes, photoinjection at the interface coupled with photoconductivity in the bulk LCP, is proposed which reproduces the experimental results.

Introduction

A number of groups have employed molecular semiconductors such as porphyrins[1] and phthalocyanines[2] in photovoltaic cells,[3-7] photoelectrochemical cells,[8-13] and electrophotographic applications.[14,15] The large visible extinction coefficients, low processing costs, and the possibility of continued improvement in performance through synthetic variation make molecular semiconductors potentially useful materials for a number of photoelectronic applications. We have recently reported the synthesis of a number of porphyrin liquid crystals[16,17] and have investigated the effect of increasing order on their photophysical properties.[18] Liquid crystals (LCs)[19-21] have an inherent tendency toward self-

(1) For a review, see: (a) *The Porphyrins*; Dolphin, D., Ed.; Academic Press: New York, 1978; Vol. I–VII. (b) *Porphyrins, Excited States and Dynamics*; Gouterman, M.; Rentzepis, P. M.; Straub, K. D., Eds.; ACS Symposium Series 321; American Chemical Society: Washington, DC, 1986.

(2) For a review, see: Moser, F. H.; Thomas, A. C. *The Phthalocyanines*; CRC Press: Boca Raton, FL, 1983; Vols. I and II.

(3) (a) Hopf, F. R.; Whitten, D. G. In ref 1a, Vol. II. (b) Felton, R. H. In ref 1a, Vol. III. (c) Davis, D. G. In ref 1a, Vol. III. (d) Loutfy, R. O.; Hsiao, C. K.; Ho, R. *Can. J. Phys.* **1983**, *61*, 1416. (e) Menzel, E. R.; Loutfy, R. O. *Chem. Phys. Lett.* **1980**, *72*, 522. (f) Martin, M.; Andre, J.-J.; Simon, J. *Nouv. J. Chim.* **1981**, *5*, 485. (g) Yamashita, K.; Harima, Y.; Iwashima, H. J. *J. Phys. Chem.* **1987**, *91*, 3055. (h) Kampas, F. J.; Gouterman, M. *J. Phys. Chem.* **1977**, *81*, 690. (i) Stanberry, B. J.; Gouterman, M.; Burgess, R. M. *J. Phys. Chem.* **1985**, *89*, 4950. (j) Tanimura, K.; Kawai, T.; Sakata, T. *J. Phys. Chem.* **1980**, *84*, 751. (k) Wang, J. H. *Proc. Natl. Acad. Sci. U.S.A.* **1969**, *62*, 653. (l) Harima, K.; Yamashita, K. *J. Phys. Chem.* **1985**, *89*, 5325. (m) Panayotatos, P.; Parikh, D.; Sauers, R.; Bird, G.; Piechowski, A.; Husain, S. *Solar Cells* **1986**, *18*, 71. (n) Tollin, G.; Kearns, D. R.; Calvin, M. *J. Chem. Phys.* **1960**, *32*, 1013.

(4) (a) Fan, F.-R.; Faulkner, L. R. *J. Chem. Phys.* **1978**, *69*, 3334. (b) Fan, F.-R.; Faulkner, L. R. *J. Chem. Phys.* **1978**, *69*, 3341.

(5) (a) Loutfy, R. O.; Sharp, J. H.; Hsiao, C. K.; Ho, R. *J. Appl. Phys.* **1981**, *52*, 5218. (b) Loutfy, R. O.; Sharp, J. H. *J. Chem. Phys.* **1979**, *71*, 1211. (c) Loutfy, R. O.; Hsiao, C. K. *Can. J. Phys.* **1981**, *59*, 727.

(6) Tang, C. W.; Albrecht, A. C. *J. Chem. Phys.* **1975**, *62*, 2139.

(7) Ghosh, A. K.; Morel, D. L.; Feng, T.; Shaw, R. F.; Rowe, C. A. *J. Appl. Phys.* **1974**, *45*, 230.

(8) (a) Jaeger, C. D.; Fan, F.-R. F.; Bard, A. J. *J. Am. Chem. Soc.* **1980**, *102*, 2592. (b) Giraudeau, A.; Fan, F.-R. F.; Bard, A. J. *J. Am. Chem. Soc.* **1980**, *102*, 5137. (c) Buttner, W. J.; Riecke, P. C.; Armstrong, N. R. *J. Phys. Chem.* **1985**, *89*, 1116. (d) Buttner, W. J.; Riecke, P. C.; Armstrong, N. R. *J. Am. Chem. Soc.* **1985**, *107*, 3738. (e) Inganas, O.; Lundstrom, I. *J. Appl. Phys.* **1983**, *54*, 4185. (f) Leempoel, P.; Fan, F.-R. F.; Bard, A. J. *J. Phys. Chem.* **1983**, *87*, 2948. (g) Klofta, T. J.; Danziger, J.; Lee, P.; Pankow, J.; Nebesny, K. W.; Armstrong, N. R. *J. Phys. Chem.* **1987**, *91*, 5646.

(9) Fan, F.-R. F.; Faulkner, L. R. *J. Am. Chem. Soc.* **1979**, *101*, 4779.

(10) Loutfy, R. O.; McIntyre, L. F. *Can. J. Chem.* **1983**, *61*, 72.

(11) Kearns, D. R.; Tollin, G.; Calvin, M. *J. Chem. Phys.* **1960**, *32*, 1020.

(12) Klofta, T. J.; Rieke, P. C.; Linkous, C. A.; Buttner, W. J.; Nanthakumar, A.; Mewborn, T. D.; Armstrong, N. R. *J. Electrochem. Soc.* **1985**, *132*, 2134.

(13) Kampas, F. J.; Yamashita, K.; Fajer, J. *Nature* **1980**, *284*, 40.

(14) (a) Hackett, C. F. *J. Chem. Phys.* **1971**, *55*, 3178. (b) Meier, H.; Albrecht, W. *Ber. Bunsen-Ges. Phys. Chem.* **1969**, *73*, 86.

(15) Law, K.-Y. *J. Phys. Chem.* **1988**, *92*, 4226.

(16) Gregg, B. A.; Fox, M. A.; Bard, A. J. *J. Chem. Soc., Chem. Commun.* **1987**, 1143.

(17) Gregg, B. A.; Fox, M. A.; Bard, A. J. *J. Am. Chem. Soc.* **1989**, *111*, 3024.

(18) Gregg, B. A.; Fox, M. A.; Bard, A. J. *J. Phys. Chem.* **1989**, *93*, 4227.

0022-3654/90/2094-1586$02.50/0

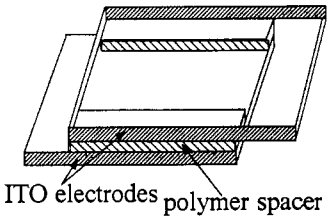

Figure 1. Schematic diagram of an emtpy LCP cell. The cell is filled by placing a few milligrams of LCP at the opening and heating to the isotropic liquid phase whereupon the porphyrin capillary-fills into the cell. It is then cooled through the liquid crystalline phase into the solid state.

organization; these LC porphyrins were synthesized in order to prepare thin, large area arrays of ordered porphyrins for the purpose of studying their photophysical, photovoltaic, and photoelectrochemical properties. Increased crystallinity has often improved the photoelectronic properties of organic thin films,[12,15,22,23] although some counterexamples have been reported.[13,25]

We report here an unusual photovoltaic effect in symmetrical cells filled with a liquid crystal porphyrin (LCP). These cells consisted of an LCP capillary-filled between two pieces of indium–tin oxide (ITO) coated glass separated by polymer spacers (see Figure 1). Upon illumination of either electrode, a substantial and stable photovoltage and/or photocurrent was generated. The illuminated electrode was always negative; short-circuit photocurrents up to 0.4 mA/cm^2 were generated under illumination with a 150-W Xe lamp. These cells showed photovoltaic characteristics comparable to some of the better organic solar cells[3-7] even though they were completely symmetrical and relatively thick (1–6 μm). Thus, we investigated the mechanism of this photovoltaic effect and developed a model that describes this behavior.

Background

Given the unexpected nature of some of our results, e.g., the generation of large photocurrents from cells that have no apparent driving force for charge separation, we considered it advantageous to include a brief review of several aspects of molecular semiconductors that will be pertinent to our discussion. The differences between the molecular semiconductors and the better understood inorganic semiconductors have often been noted.[24,26-28] One of the primary physical differences between organic (or van der Waals bonded) semiconductors and inorganic (or covalently bonded) semiconductors is the extent of orbital overlap along the conducting pathway.[26,29] Covalently bonded semiconductors commonly have an orbital overlap that results in a bonding interaction on the order of several eV.[29-32] As a consequence of this large lattice interaction, deviations from crystal perfection strain or break covalent bonds, leading to energetic states distributed throughout the otherwise forbidden bandgap.[29,32] Furthermore, substitutional impurities of a valence different from that of the host can give rise to free charge carriers. Thus, minute quantities of impurities or lattice imperfections can change an otherwise insulating material (e.g., TiO_2, ZnO) into a semiconductor.[29] As a result of both the large lattice forces and the generally high dielectric constants of inorganic semiconductors, light absorption usually leads to the direct formation of free electron–hole pairs.[29]

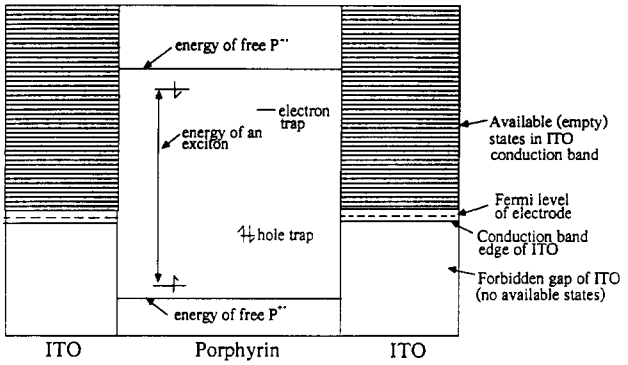

Figure 2. Schematic diagram of the energy of a singlet exciton relative to the energy levels of the free carriers and to the ITO electrodes in an LCP cell. The energy of an exciton is less than that required to generate free carriers primarily due to the electrostatic attraction between opposite charges in a medium of low dielectric constant. As shown, the only isoenergetic dissociation pathway for excitons is injection of an electron into the empty states of the ITO conduction band. A free carrier can also be generated by the interaction of an exciton with a trap.

In contrast, most organic materials have an intermolecular orbital overlap on the order of 0.1 eV.[24,26] Therefore, the properties of the solid are only slightly perturbed from those of the monomers, and a correct description of the solid must emphasize molecular, rather than collective, properties. Absorption of a photon in these materials usually leads to the formation of a Frenkel (i.e., strongly bound) exciton rather than an electron–hole pair.[24,26] Because of the weak lattice forces, crystal dislocations, surfaces, and impurities often cause relatively small perturbations in energy which do not give rise to free charge carriers. For example, carbazole impurities create a trap depth of only 0.034 eV in anthracene crystals.[26a] Therefore, although the defect density and impurity level in molecular semiconductors are often greater than those in inorganic semiconductors, the charge carrier density is often much smaller in the organic compound compared to an inorganic compound of similar band gap.[24,26,29]

These differences between molecular and inorganic semiconductors have several implications for the design of organic solar cells. In the usual Schottky barrier solar cell, the semiconductor is sandwiched between a (dark) ohmic and an (illuminated) blocking contact.[32-34] However, the formation of either a blocking or an ohmic contact, which requires that the semiconductor come to electrochemical equilibrium with its electrodes,[29] is questionable

(19) (a) *Liquid Crystals and Plastic Crystals*; Gray, G. W., Winsor, P. A., Eds.; Wiley: New York, 1974; Vols. I and II. (b) *Advances in Liquid Crystals*; *Brown*, G. H., Ed.; Academic Press: New York, 1975–1983; Vol. 1–6.

(20) (a) Chandrasekhar, S. *Mol. Cryst. Liq. Cryst.* **1981**, *63*, 171. (b) Destrade, C.; Tinh, N. H.; Gasparoux, H.; Malthete, J.; Levelut, A. M. *Mol. Cryst. Liq. Cryst.* **1981**, *71*, 111. (c) Dubois, J. C.; Billard, J. In *Liquid Crystals and Ordered Fluids*; Griffin, A., Johnson, J. F., Eds.; Plenum Press: New York, 1984; Vol. 4.

(21) (a) Piechocki, C.; Simon, J.; Skoulios, A.; Guillon, D.; Weber, P. *J. Am. Chem. Soc.* **1982**, *104*, 5245. (b) Knoesel, R.; Piechocki, C.; Simon, J. *J. Photochem.* **1985**, *29*, 445. (c) Blanzat, B.; Barthou, C.; Tercier, N.; Andre, J.-J.; Simon, J. *J. Am. Chem. Soc.* **1987**, *109*, 6193. (d) Markovitsi, D.; Tran-Thi, T.-H.; Briois, V.; Simon, J.; Ohta, K. *J. Am. Chem. Soc.* **1988**, *110*, 2001.

(22) Hor, A. M.; Loutfy, R. O. *Thin Solid Films* **1983**, *106*, 291.

(23) LeBlanc, O. H. In ref 24, Vol. III.

(24) *Physics and Chemistry of the Organic Solid State*; Fox, D., Labes, M. M., Weissberger, A., Eds.; Interscience: New York, 1963, 1965, 1967; Vols. I–III.

(25) Morel, D. L.; Stogryn, E. L.; Ghosh, A. K.; Feng, T.; Purwin, P. E.; Shaw, R. F.; Fishman, C.; Bird, G. R.; Piechowski, A. P. *J. Phys. Chem.* **1984**, *88*, 923.

(26) (a) Pope, M.; Swenberg, C. E. *Electronic Processes in Organic Solids*; Oxford University Press: New York, 1982. (b) Simon, J.; Andre, J.-J.; *Molecular Semiconductors*; Springer Verlag: Berlin, 1985. (c) Gutman, F.; Lyons, L. E. *Organic Semiconductors, Part A*; Krieger: Malabar, FL, 1981. (d) Gutmann, F.; Keyser, H.; Lyons, L. E. *Organic Semiconductors, Part B*; Krieger: Malabar, FL, 1983.

(27) Kommandeur, J. *J. Phys. Chem. Solids* **1961**, *22*, 339.

(28) Twarowski, A. J.; Albrecht, A. C. *J. Chem. Phys.* **1979**, *70*, 2255.

(29) Smith, R. A. *Semiconductors*, 2nd ed.; Cambridge University Press: Cambridge, 1978.

(30) (a) Marks, T. J. *Science* **1985**, *227*, 881 and references therein. (b) Ciliberto, E.; Doris, K. A.; Pietro, W. J.; Reisner, G. M.; Ellis, D. E.; Fragala, I.; Herbstein, F. H.; Ratner, M. A.; Marks, T. J. *J. Am. Chem. Soc.* **1984**, *106*, 7748.

(31) Whangbo, M. H. *Acc. Chem. Res.* **1983**, *16*, 95.

(32) Blakemore, J. S. *Solid State Physics*, 2nd ed.; Saunders: Philadelphia, 1974.

(33) *Semiconductor Liquid-Junction Solar Cells*; Heller, A., Ed.; Electrochemical Society: Princeton, 1977.

(34) *Thin Film Solar Cells*; Chapra, K. L., Das, S. R., Eds.; Plenum Press: New York, 1983.

in the case of many organic systems.[35] Ohmic contacts to anthracene, the most well-studied organic crystal, have been achieved only with strongly oxidizing contacts, e.g., Ce^{3+}/Ce^{4+} in H_2SO_4,[26a,36] or solid $Ce(SO_4)_2$,[23] which are ohmic for holes, or with the strongly reducing contact, sodium anthracenide in THF,[36] which is ohmic for electrons. Thus, the formation of an ohmic contact to an anthracene crystal apparently requires a redox potential (Fermi level[37]) close to the potential for either the oxidation or the reduction of anthracene.[26a] No metal films have been found to form ohmic contacts with anthracene.[23,38] Similarly, the formation of a blocking contact requires that the thickness of the resulting space charge layer, L_{sc}, be less than the cell thickness.[39] This would commonly require[39] a charge carrier density of greater than approximately 10^{14} cm^{-3}. However, the carrier density in single-crystal phthalocyanines and anthracene is on the order of 10^4–10^7 cm^{-3}.[26c,35]

Such examples suggest that molecular semiconductors may often not come to equilibrium with their electrodes, in which case the photovoltaic properties will not be directly determined by the work functions of the contacts. Rather, evidence now suggests that, at least in single-crystal materials, exciton migration to the surface, followed by dissociation and injection of one carrier into the electrode, is often the dominant mechanism for photocurrent production.[24,26,27] A characteristic feature of molecular semiconductors is that the band gap lies higher in energy than the optical absorption edge;[35] i.e., it is not energetically feasible for a Frenkel exciton formed in the organic layer by long-wavelength excitation to dissociate into both a free electron and a free hole without some additional energy input. Thus, the exciton may freely diffuse in the bulk of the crystal. However, if the available electrode energy levels lie far enough inside the band gap (Figure 2), it is possible for an exciton, upon reaching the surface, to inject *one* carrier into the electrode[26] leaving behind a free carrier in the organic layer. Exciton interaction with deep trap sites in the bulk can also give rise to one free and one trapped carrier. In several cases, direct generation of electron–hole pairs in the bulk has been reported when exciting into states lying higher in energy than the first singlet.[26a,40,41]

The first photovoltaic effect in an organic crystal sandwiched between identical electrodes was reported by Kallman and Pope[42] using 5-μm-thick single crystals of anthracene to separate two aqueous NaCl solutions. Upon illumination, a photovoltage of up to 200 mV was generated, the illuminated side being negative. A photovoltage cannot be generated merely by an increase in the number of free carriers near an illuminated interface;[43] thus, they concluded that charge transfer across the illuminated interface must occur by a different mechanism than charge transfer across the dark interface.

Hall et al.[44] studied the effect of different metal electrodes on the performance of phthalocyanine solar cells that were prepared and studied under vacuum. Significantly, for *all* cells, the illuminated electrode charged negative and V_{oc} was between −0.2 and −0.4 V. This was true for M_1, M_2 = Al, Au; Au, Al; Au, Au; and Al, Al as well as for the Pb electrodes, where M_1 was the illuminated electrode and M_2 the dark electrode.

Geacintov et al.[40] studied the photogeneration of charge carriers under a voltage bias in ca. 20-μm-thick tetracene single crystals sandwiched between two distilled water electrodes. They concluded that most of the photocurrent was produced by exciton diffusion to the illuminated interface followed by hole injection into the tetracene. A much smaller percentage of the current originated from bulk generation of carriers. When the exciting light was scanned toward shorter wavelengths, the fluorescence quantum yield decreased while the photocurrent from bulk generated carriers increased. They derived an expression for the hole injection current, i^+:

$$i^+ = eI_0\Phi_{ex(\lambda)}A\left(\frac{\alpha L}{\alpha L + 1}\right) \quad (1)$$

where $\Phi_{ex(\lambda)}$ is the wavelength-dependent quantum yield for exciton formation (assumed to be proportional to the quantum yield for fluorescence), A is the maximum efficiency for charge carrier production, α is the absorption coefficient, and L is the exciton diffusion length. From this analysis they calculated that L = 2000 Å.

Experimental Section

Zinc octakis(β-octyloxyethyl)porphyrin (ZnOOEP) and its other metallo and free-base derivatives were prepared and purified as described previously.[17] The substrate for the cells was indium–tin oxide (ITO) coated float glass from Delta Technologies. The glass was cut into 1 cm × 1.5 cm pieces, and the ITO was removed from a thin strip on three sides of each piece (this reduced the number of shorts in the cells) by rubbing with a cotton applicator that had been soaked in HCl/2-propanol solution and dipped in zinc dust. The glass was then cleaned by sonication in a KOH/2-propanol solution followed by copious rinsing with deionized water. It was then rinsed sequentially with 95% ethanol, distilled acetone, and reagent grade 2-propanol before being dried at 120 °C in air. The cells were prepared by spin coating a spacer solution of 4% poly(ethylene-*co*-vinyl acetate) (Scientific Polymer Products) in dichloroethane containing 20% triethylbenzene onto a masked ITO plate. Removal of the Teflon tape mask left two strips of polymer which would adhere to another ITO plate, if assembled while still tacky. The two ITO plates were offset from one another with the conducting edges on the outside to provide electrical contacts (see Figure 1). The plates were pressed together, while the spacers were still tacky, until the minimum number of optical fringes appeared across the cell, thus ensuring that the electrodes were approximately parallel. After the spacers were dried at 60 °C for ca. 1 h, the cells were sealed along the two spacer sides with epoxy cement.

The cells were then tested for electrical shorts by applying a voltage ramp from +9 to −9 V across the electrodes. If any current was detected, an ac voltage of increasing magnitude (up to ±10 V) was applied to the cells to burn out the shorts. If this was unsuccessful, the cell was discarded. These cells could be made in a thickness range of 0.8–8 μm (as measured by the optical absorption of the porphyrin-containing cells). The LC porphyrin was capillary-filled into the cell by placing ca. 1 mg of LCP at the cell opening and heating to slightly above the isotropic liquid phase (i.e., to ca. 180 °C for ZnOOEP) until the cell was full and then cooling slowly through the liquid crystalline phase to the solid. The resulting LCP phase was polycrystalline with crystallites up to several millimeters in diameter (cf. Figure 4, ref 17).

A 150-W Xe lamp (Oriel) with a 12-cm water filter was used for most of the experiments involving white light. The intensity of this source at the cell surface was ca. 150 mW/cm² (as measured on a Scientech power meter). Occasional use was made of a 1000-W Xe lamp (Oriel) with the same water filter. The incident intensity was regulated by the use of a series of calibrated wire mesh screens: 10 screens corresponded to 1.9% transmission. For monochromatic illumination, the lamp (250-W Xe with a parabolic reflector) and scanning monochromator in an SLM

(35) Lyons, L. E. In ref 24, Vol. I.
(36) Helfrich, W. In ref 24, Vol. III.
(37) Reiss, H. *J. Phys. Chem.* **1985**, *89*, 3783.
(38) Reucroft, P. J. *J. Chem. Phys.* **1962**, *36*, 1114.
(39) L_{sc} is related to the charge carrier density, N_d, by $L_{sc} \approx (1.1 \times 10^6 \Delta V \epsilon / N_d)^{1/2}$, where ΔV is the voltage drop across the space charge layer and ϵ is the dielectric constant of the semiconductor. Thus, to generate a blocking contact in a 1-μm-thick cell with ΔV = 0.2 V and ϵ = 3 requires a carrier density of greater than approximately 10^{14} cm^{-3}. See, for example: Bard, A. J. *J. Photochem.* **1979**, *10*, 59.
(40) Geacintov, N.; Pope, M.; Kallman, H. *J. Chem. Phys.* **1966**, *45*, 2639.
(41) Castro, G.; Hornig, J. F. *J. Chem. Phys.* **1965**, *42*, 1459.
(42) Kallman, H.; Pope, M. *J. Chem. Phys.* **1959**, *30*, 585.
(43) Mott, N. F.; Gurney, R. W. *Electronic Processes in Ionic Crystals*, 2nd ed.; Dover: New York, 1964; p 192.
(44) Hall, K. J.; Bonham, J. S.; Lyons, L. E. *Aust. J. Chem.* **1978**, *31*, 1661. These results were explained by assuming that all of the metals formed ohmic contacts with the phthalocyanine and that the direction of current flow was determined by a higher density of hole traps on the nonsubstrate (M_2) side of the cell. We note that these results can also be explained by assuming that the phthalocyanine does not come to equilibrium with its contacts and that electrons are injected into the electrode at whichever interface is illuminated.

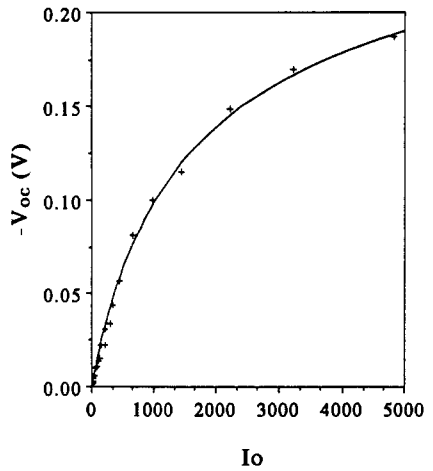

Figure 3. Dependence of the open-circuit photovoltage, V_{oc}, on the incident light intensity, I_o, at 585 nm. I_o is given in units of 10^{12} quanta s^{-1} cm^{-2}. The curve is a plot of (14) with $\Phi_{pf}^{\circ} = 0.05$, $\Phi_{nf}^{\circ} = 0.0025$, $\sigma_{ps} = 47\ \Omega^{-1}\ cm^{-2}$, $\alpha_p = 0.85$, $\alpha_n = 0.15$, and $P = 0.2$.

Aminco SPF 500 spectrofluorometer were used. The output flux of this system was calibrated with a silicon photodiode detection system (Oriel). Action spectra could be conveniently measured by feeding the short-circuit photocurrent directly from the LCP cell into the signal input of the spectrofluorometer. The action spectra were generally measured at 2-nm resolution, the lamp spectrum (measured with the Si photodiode) was then divided out, and the resulting spectra were stored on disk. This procedure was checked by also measuring action spectra with a potentiostat and a recorder: the results were identical. The current–voltage measurements were performed with a Princeton Applied Research 175 universal programmer, a Model 173 potentiostat, and a Model 179 digital coulometer. The signal was recorded on a Houston Instruments 2000 *X–Y* recorder. An Oriel 7072 detection system was also used to measure photocurrents, and voltages were also measured with a Fluka 77 multimeter. Preliminary kinetic measurements employed the lamp and the shutter (rise time ≈ 10 ms) of the spectrofluorometer while the signal was captured on a Nicolet 2090 digital oscilloscope.

Results and Discussion

The results presented here are primarily from a single porphyrin, zinc octakis(β-octyloxyethyl)porphyrin[17,18] (ZnOOEP), which is a liquid crystalline analogue of zinc octaethylporphyrin (ZnOEP). These two compounds differ only in their thermotropic behavior and solubility. Several preliminary experiments with the free-base, Mg, Cd, and Pd derivatives[17] of this liquid crystal porphyrin are also reported. *It should be emphasized that the following results concern the solid phase of the LCP; the liquid crystalline phase was used only as a means of preparing an ordered solid.*

Open-Circuit Photovoltage. Upon illumination of a cell containing a thin (1–6 μm) film of solid LCP with white light at open circuit, the illuminated electrode charged negative (the dark electrode is considered to be at ground). Typical values for the photovoltage were −150 to −350 mV. If the cell was then turned around and the opposite side illuminated, the photovoltage quickly decayed to zero and then charged negative. The increase of the open-circuit photovoltage, V_{oc}, with intensity, I_o (Figure 3), is similar to that seen in a number of organic systems.[26a,42,44,45] V_{oc} eventually saturates at high intensity: for the cell shown in Figure 3, this occurred at $V_{oc} = -0.26$ V. The dependence of V_{oc} on the wavelength (Figure 4) resembles the absorption spectrum of the cell at wavelengths longer than ca. 450 nm. At shorter wavelengths, the photovoltage is smaller than would be expected on the basis of the absorption spectrum. This decrease correlates with the decrease in the wavelength-dependent quantum yield for fluorescence measured previously.[18] Preliminary kinetic measurements showed that there were two components to the photovoltage: approximately 90% of the photovoltage has a rise and decay time faster than the shutter (ca. 10 ms), while the remaining 10% of the signal has a much longer time constant of ca. 1 s.

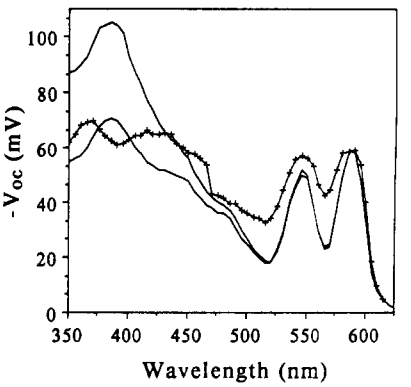

Figure 4. Dependence of the open-circuit photovoltage, V_{oc}, on the wavelength, λ, of the incident light (normalized to a flux of 1.3×10^{15} quanta s^{-1} cm^{-2}). Cell thickness was 5 μm. The slit width was 5 nm. The experimental data is shown as crosses connected by a line. The solid curves were calculated from (3) and (14) and the data in Figure 3. The exciton diffusion length was assumed to be $L = 0.25$ μm. The upper theoretical curve assumes a quantum yield $\Phi_{ex(\lambda)} = 1$ for all wavelengths; the lower theoretical curve uses the $\Phi_{ex(\lambda)}$ measured in ref 18.

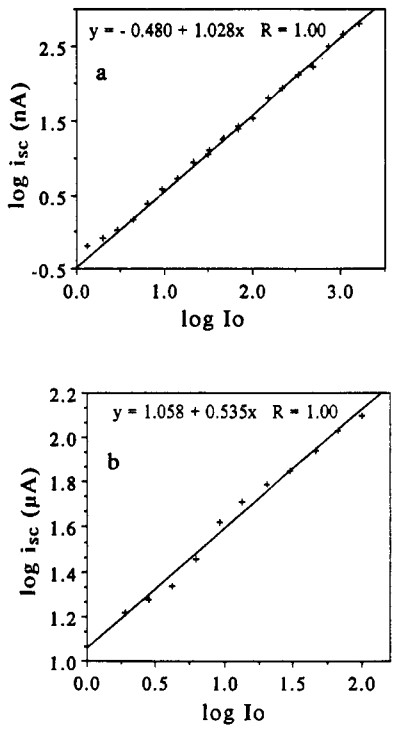

Figure 5. Dependence of the short-circuit photocurrent, i_{sc}, on the incident intensity, I_o. Cell area was 0.25 cm^2. (a) Monochromatic light at λ = 400 nm; I_o is in units of 10^{12} quanta s^{-1} cm^{-2}. (b) White light; I_o is in units of ca. 20 mW/cm^2. The lines give the best fit to the data; R is the correlation coefficient.

Short-Circuit Photocurrent. The dark current of the LCP cells was below our limits of detection up to a field strength of ca. 5×10^4 V/cm, i.e., the apparent dark resistivity was greater than 10^{13} Ω cm. Upon illumination, the light electrode acted as a photoanode. As with the photovoltage, the photocurrent would reverse direction if the cell was illuminated from the opposite side. The short-circuit photocurrent, i_{sc}, was a linear function of the light intensity over more than 3 orders of magnitude (Figure 5a), up to the highest available values of monochromatic light (ca. 10^{15} photons s^{-1} cm^{-2}). This linearity was independent of the exciting wavelength; that is, the normalized action spectra measured at different intensities were superimposable. The photocurrent under an applied bias was also linear with intensity in this range. At much higher intensities (white light, >ca. 20 mW cm^{-2}), i_{sc} in-

(45) Bonham, J. S. *Aust. J. Chem.* **1976**, *29*, 2123.

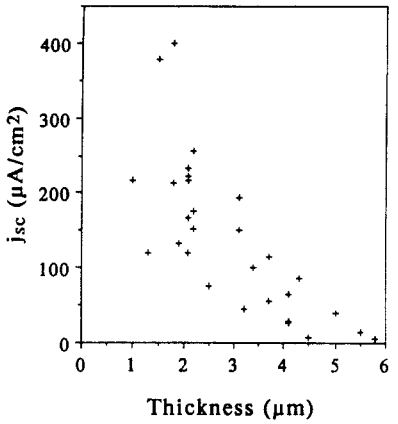

Figure 6. Dependence of the short-circuit-photocurrent density, j_{sc}, on cell thickness for 29 ZnOOEP cells.

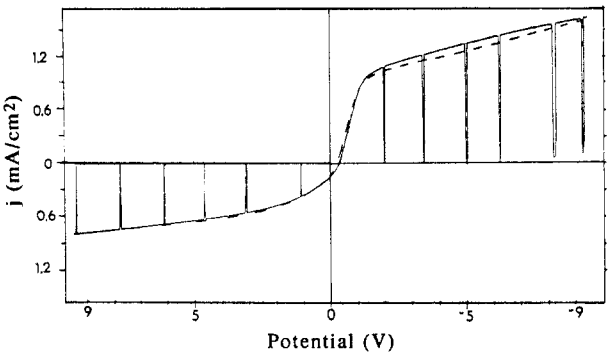

Figure 7. Typical photocurrent–voltage curve for an LCP cell. The scan originated at −9.5 V, scanned to +9.5 V (solid line) and then back to −9.5 V (dashed line) showing a slight hysteresis. The scan rate was 100 mV/s. Illumination was with white light of ca. 150 mW/cm². The vertical lines show where the light was chopped manually. Cathodic currents are plotted up.

creased with the square root of the intensity (Figure 5b). The short-circuit photocurrents were quite stable. After an initial decay of ca. 15%, i_{sc} remained constant under illumination of 150 mW/cm² for 72 h (corresponding to the passage of ca. 10^4 electrons per porphyrin) in the two cells so tested. Preliminary kinetic results showed that both the rise and decay of the photocurrent occurred with time constants faster than ca. 10 ms.

Photocurrent vs Thickness. The short-circuit-photocurrent density, j_{sc}, was a strong function of the cell thickness, d (Figure 6). There was, however, a large variation in j_{sc} from cell to cell resulting from a number of factors such as the length of time that the porphyrin was molten during capillary-filling (heat was detrimental to j_{sc}) and the number of shorts that had to be burned out of the empty cell before filling (this also decreased j_{sc}). Furthermore, most of the cells that were thinner than ca. 2 μm were shorted to some degree after filling; i.e., they exhibited some amount of dark current which was linear with voltage. Presumably these shorts decreased both the measured V_{oc} and j_{sc}. Typical values for the short-circuit-photocurrent density (under white light illumination of ca. 150 mW/cm²) were j_{sc} = 15 μA/cm² for a 5-μm-thick cell and j_{sc} = 250 μA/cm² for a 1.5-μm-thick cell.

Photocurrent vs Voltage. The dependence of the photocurrent on the applied voltage (Figure 7) showed a characteristic S-shaped curve displaced from the origin by $V = V_{oc}$. The photocurrent increased very rapidly with voltage around $V = V_{oc}$ and eventually decreased to a linear function at higher voltage. The photocurrent in the linear region was always 2–3 times as high for negative voltages applied to the illuminated electrode as for positive.

Photocurrent vs Wavelength. The dependence of the short-circuit photocurrent on the wavelength of the incident light (Figure 8) was a function of cell thickness. For very thin cells (ca. 1 μm), the action spectrum resembled the absorption spectrum. However, for thick cells (ca. 5 μm), the photocurrent showed a valley for every peak in the absorption spectrum. The action spectra changed

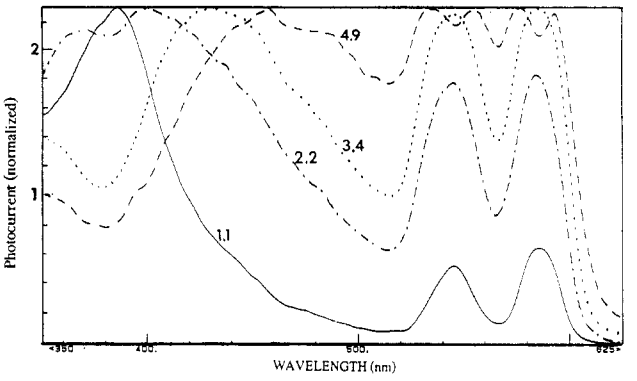

Figure 8. Dependence of the short-circuit photocurrent, i_{sc}, on the wavelength of the exciting light (action spectra) for different cell thicknesses. The slit width was 2 nm; the currents are normalized at the highest point. The numbers on the curves give the cell thickness in μm. The solid line (d = 1.1 μm) corresponds closely to the absorption spectrum of an LCP cell.

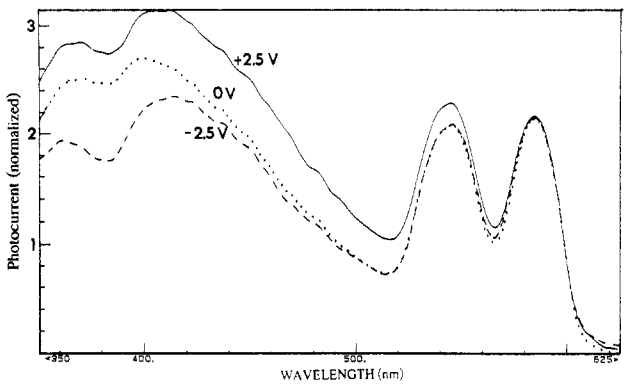

Figure 9. Dependence of the action spectra on the applied voltage. The cell thickness was 2.2 μm. The slit width was 2 nm; the current was normalized at 585 nm. The numbers on the curves give the applied voltage.

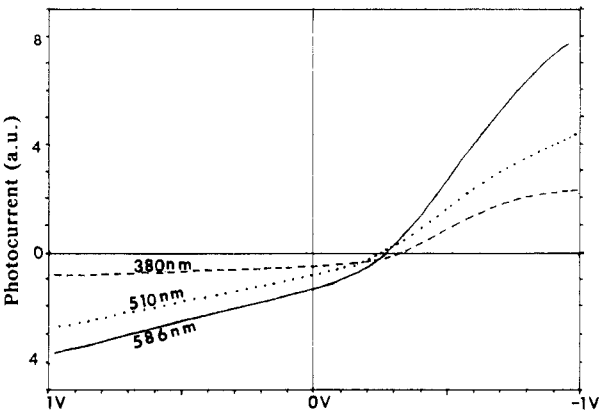

Figure 10. Photocurrent–voltage curves as a function of incident wavelength. Cell was 3.4 μm thick; slit width was 5 nm. Excitation wavelengths are indicated on the curves. Cathodic currents are plotted upward. Absorption coefficients are α = 1.8 μm^{-1} at 380 nm, α = 0.10 μm^{-1} at 510 nm, and α = 0.45 μm^{-1} at 586 nm.

only slightly when measured under positive, zero, or negative bias (Figure 9; the applied field strength was 1.1 × 10^4 V/cm). The wavelength dependence of the photocurrent is also apparent in the i–V scans (shown for a 3.4-μm-thick cell; Figure 10); the most strongly absorbed wavelength (380 nm, α = 1.8 μm^{-1})[46] led to the largest photovoltage but to the smallest j_{sc} and limiting current. Less strongly (but still almost completely) absorbed light (586 nm, α = 0.45 μm^{-1}) led to a slightly smaller V_{oc} but to much larger

(46) The absorption coefficients, α, quoted in the text are to the base 10; those used in the calculations were, of course, the exponential.

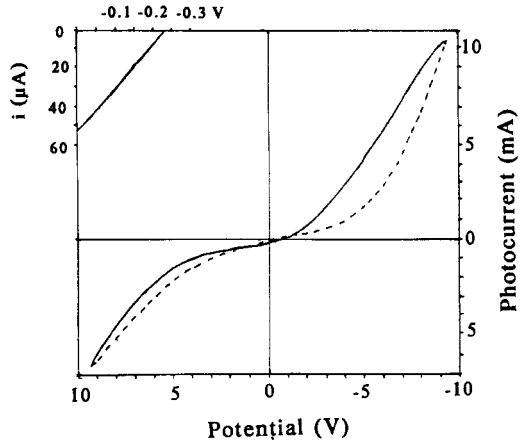

Figure 11. Photocurrent–voltage (i–V) curve and power curve (inset in the second quadrant) of a ZnOOEP cell containing ca. 2 mol % DDQ. The cell was 0.3 cm² × 2.4 μm. The solid line in the i–V plot is the original scan from −9.6 to +9.6 V; the dashed line is the reverse scan. The scan rate was 100 mV/s for the i–V curve and 2 mV/s for the power curve.

limiting currents. Light of a wavelength that was not completely absorbed by the cell (510 nm, $\alpha = 0.10\ \mu m^{-1}$) gave a still smaller photovoltage and a limiting current intermediate between the other two.

Effect of Dopants. The effects of O_2 and other acceptors on the conductivity of porphyrins and phthalocyanines have been widely discussed.[11,26,47-49] In most of our experiments no attempt was made to exclude oxygen, although its concentration was presumably low since the cells were capillary-filled at ca. 180 °C. In one set of experiments, however, the LCP was first dissolved in benzene and N_2 was bubbled through the solution for 1 h before the solvent was evaporated, still under N_2. Two cells, both 2.1-μm-thick that had been stored under vacuum at 100 °C, were filled with this N_2-treated ZnOOEP. Then the procedure was repeated, but O_2 was bubbled through the LCP solution. Again, two cells (2.1 and 1.9 μm thick) were filled with this O_2-treated LCP. The two N_2-treated cells showed j_{sc} = 222 and 233 μA/cm² and V_{oc} = −220 and −230 mV while the two O_2-treated cells showed j_{sc} = 133 and 167 μA/cm² and V_{oc} = −180 and −200 mV. This indicates that O_2 might be detrimental to the cell performance, although the large cell-to-cell variability (see Figure 6) makes this conclusion uncertain. However, *O_2 is certainly not required for the photovoltaic effect.* Addition of any one of a number of other oxidants (ca. 1–10 mol % of I_2, *o*- and *p*-chloranil, TCNQ) to the porphyrin phase had almost no measurable effect on the photoproperties. However, the addition of DDQ (dichlorodicyano-*p*-benzoquinone, ca. 1–10 mol %) to the LCP led to a 20–50-fold increase in the limiting photocurrent under a bias, although the short-circuit photocurrent and open-circuit photovoltage were not greatly affected. The power curves of DDQ-doped cells were similar to undoped cells; however, the shape of the i–V curves at higher voltage was qualitatively different (Figure 11). The current did not reach a limiting plateau in the accessible voltage range, and it exhibited a substantial hysteresis.

Other LC Porphyrins. Photoeffects observed with the Mg, Cd, or Pd derivatives of the liquid crystal porphyrin (data not shown) were completely analogous to the ZnOOEP cells, although the photocurrents were smaller by factors of 2–5. This may be related to the fact that, having been synthesized in much smaller quantities, they were probably not as pure as the ZnOOEP. Although the potentials for oxidation of the Mg and Cd compounds are ca. 200 mV negative of ZnOOEP, and that of the Pd compound is ca. 200 mV positive of ZnOOEP, the open-circuit photovoltage

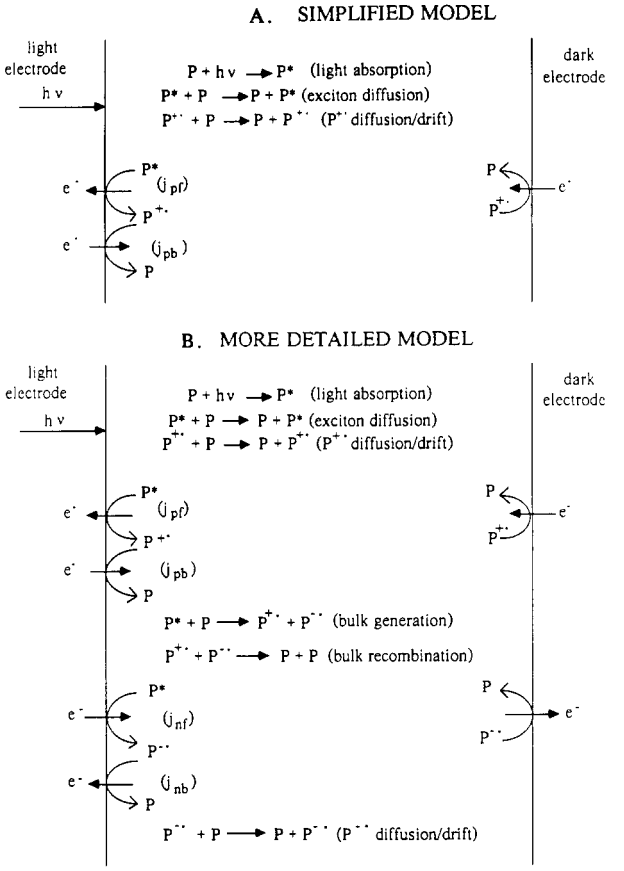

Figure 12. Simplified (A) and more detailed (B) models of the photovoltaic behavior of LCP cells.

generated in these cells was essentially the same as that in the ZnOOEP cells. A number of cells were also made from the free-base derivative, H_2OOEP. Although the photovoltage in these cells was of the same magnitude as that from the other cells, the photocurrent was approximately 3 orders of magnitude lower than with the metallo derivatives. As we reported previously,[17] the porphyrin's central metal plays an important role in mesophase formation and H_2OOEP has only a small liquid crystalline range (<5 °C). This is perhaps responsible for the very small size of the crystallites in the H_2OOEP cells, compared to the metalloporphyrin cells, and could be the cause of their low photoconductivity.

The LCP Model

An exact analysis of the photovoltaic behavior of these LCP cells is difficult. However, we have developed a simple model that shows the essential features of our results. As opposed to the model used for most photocells, where charge separation is produced by a gradient of electrochemical potential, *the model assumed here is based on the differential kinetics of hole vs electron injection at the illuminated interface.* The model thus resembles, in some aspects, both the mechanism of a photogalvanic cell[50] and the sensitization of semiconductor electrodes.[51] We assume that, with no applied bias, the preferential photoinjection of one carrier (electrons) into the illuminated electrode is responsible for the asymmetry developed upon illumination of these symmetrical cells. This can be rationalized as resulting from the greater orbital overlap of the exciton energy level with the empty, compared with the filled, conduction-band states in the ITO electrode (Figure 2). This assumption, together with the assumption that the porphyrin does not come to equilibrium with its electrodes in the dark, can predict the development of a photovoltage in these cells and its insensitivity both to the redox potential of the porphyrin and to the presence of dopants. These assumptions can fur-

(47) Klofta, T. J.; Sims, T. D.; Pankow, J. W.; Danziger, J.; Nebesny, K. W.; Armstrong, N. R. *J. Phys. Chem.* **1987**, *91*, 5651.
(48) (a) Kaufhold, J.; Hauffe, K. *Ber. Bunsen-Ges. Phys. Chem.* **1965**, *69*, 168. (b) Meier, H.; Albrecht, W.; Tschirwitz, U. *Ber. Bunsen-Ges.* **1969**, *73*, 795.
(49) Bourdon, J.; Schnuriger, B. In ref 24, Vol. III.
(50) See, for example: Albery, J. W. *Acc. Chem. Res.* **1982**, *15*, 142.
(51) See, for example: Gerischer, H. *Photochem. Photobiol.* **1972**, *16*, 243.

thermore explain the results of Hall et al.[44] mentioned previously and are also compatible with the results of a number of other workers.[23,35,36,38,42]

Thus, in a simplified model (Figure 12A), an exciton that reaches the ITO surface injects an electron into the ITO leaving behind a radical cation ($P^{\bullet+}$) that can formally be considered a hole in the LCP. The photocurrent arises from the transport of $P^{\bullet+}$, presumably by a hopping mechanism, to the dark electrode where an electron is injected into the LCP to form the neutral porphyrin, P. However, the action spectra cannot be explained solely on the basis of photoinjection. If the photocurrent were limited only by the rate of photoinjection, the action spectra would resemble the absorption spectrum and be independent of thickness[23] (assuming an absence of space charge effects and recombination; see below). We can explain the action spectra of the LCP cells by assuming that *both* carrier injection at the surface *and* bulk generation of carriers take place, the spectral dependence of the photocurrent being determined by the interaction of these two processes. The resistance of the cell is thus dependent on the number and spatial distribution of the bulk generated carriers.

Figure 12B, a more detailed model, shows a diagram of the various processes that we assume are occurring in the illuminated LCP cells. These are light absorption and exciton flux to the front electrode; carrier injection at the illuminated interface (resulting in hole and electron injection current densities, j_{pf} and j_{nf}, respectively); recombination at the illuminated interface (j_{pb} and j_{nb}, respectively); carrier transport through the cell; the discharge of $P^{\bullet+}$ and $P^{\bullet-}$ at the dark electrode; the generation of $P^{\bullet+}$ and $P^{\bullet-}$ through an exciton intermediate in the bulk; and bulk recombination (the reaction of $P^{\bullet+}$ with $P^{\bullet-}$). We assume that the discharge of the species reaching the dark electrode is a fast process that does not limit the current flow, and therefore we do not consider it further. Also, since the absorbance of the LCP is high and the diffusion length of the exciton is small,[26,40] we neglect the effect of excitons reaching the back surface. We further assume that the rates of any injection processes occurring in the dark are negligible compared to the rates of the light processes. Finally, we neglect the effect of traps except insofar as they promote the generation of carriers in the bulk.

Circuit Model. We restrict our attention to the steady-state behavior of these cells. We first discuss the case in which no external voltage is applied to the cell; this is the "power curve" region, that is, between zero and the open-circuit photovoltage (corresponding to photocurrents between the short-circuit photocurrent and zero, respectively). Our model considers that the action of light on the LCP cell is to inject charge into the ITO electrode, so that *the organic layer becomes electrostatically charged relative to the electrode.* This is modeled as being equivalent to the charging of a capacitor by a photocurrent source whose rate of carrier injection, j_f, is a function of both the incident light intensity and the interfacial voltage, V_c. Thus, we propose to model the LCP cells as the equivalent circuit shown in Figure 13. The charge injected into the ITO and the opposite charge in the LCP layer create a charged bilayer at the interface, modeled by the capacitance, C. The recombination rate of the injected species is assumed to be governed by the shunt resistance, R_s, and thus is directly proportional to the interfacial voltage, V_c (recombination rate = $i_b = V_c/R_s$). V_c, in turn, is directly proportional to the number of injected carriers ($V_c = q/C$). At open circuit, the injection rate must equal the recombination rate. When the circuit is closed, some of the injected charge traverses the cell (with an effective resistance, R) and is discharged at the dark electrode.

Summing the voltage drops around the equivalent circuit (Figure 13) leads to

$$V + iR - V_c = 0 \qquad (2)$$

where V is the measured voltage between the two electrodes (the dark electrode is considered to be at ground), i is the current through the cell, R is the cell resistance, and V_c is the voltage on the capacitor, i.e., the voltage drop across the illuminated interface (*V_c is not directly measurable, except at open circuit* where $V = V_{oc} = V_c$). It is this voltage, V_c, that controls both the rate of photoinjection and the rate of recombination. When a current flows, the observable voltage, V, will consist of both the interfacial voltage, V_c, and the voltage drop caused by the electrical resistance of the organic layer, iR. When expressed in terms of the measurable voltage, V, the problem is nonlinear, since that fraction of the voltage which controls the interfacial current, V_c, is a function of the current (see (17) below). This situation is analogous to that involved in performing electrochemical measurements in a very resistive medium without the use of a reference electrode. In the usual electrochemical setup, a reference electrode is positioned close to the working (in our case, the illuminated) electrode; thus V_c is measured directly. In the LCP cells this was not possible.

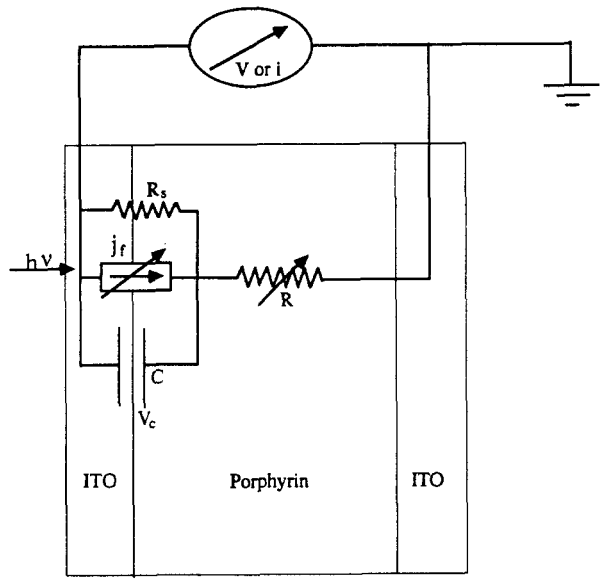

Figure 13. Equivalent-circuit model of an LCP cell. The injection process is modeled as a variable current source, j_f, in parallel with a capacitance, C, and a shunt resistance, R_s. Photocurrents flow through the variable bulk resistance, R. j_f is assumed to be a function of both the incident light intensity and the interfacial voltage, V_c.

All four of the electron-transfer reactions occurring at the illuminated interface (Figure 12B) are chemically irreversible. $P^{\bullet+}$ and $P^{\bullet-}$ production (j_{pf} and j_{nf}, respectively) involve an excited-state reactant (an exciton) and result in a ground-state (oxidized or reduced) product. Back electron transfer to form the excited state would be highly improbable. The back-reaction of holes (j_{pb}) and electrons (j_{nb}) at the illuminated electrode involve oxidized or reduced porphyrin as the reactant and the neutral porphyrin as the product. We assume that the reverse reactions (i.e., dark injection) occur at negligible rates because the dark currents in these cells were below our limits of detection. Since each of the four reactions is irreversible, the cell potential is not governed by thermodynamics; rather the cell is a "mixed potential" system. Thus, all of the reactions are referenced to the zero of applied voltage, i.e., to the short-circuit condition.

Simple Model: Neglect of Bulk Resistance and Bulk Carrier Generation. Hole Injection. We first treat the simplest case (Figure 12A) in which (1) only a single carrier is photoinjected, producing $P^{\bullet+}$; (2) no carriers are generated in the bulk; and (3) the resistance of the bulk is negligible (i.e., transport of $P^{\bullet+}$ to the dark electrode is very fast). *This last condition means that* $V_c = V$. Under these conditions, the maximum possible hole current is simply given by the maximum exciton flux to the illuminated electrode. Following Geacintov et al.[40] (see (1)), we can write an expression for the maximum probability, P, that an exciton generated in the bulk will reach the surface:

$$P = \Phi_{ex(\lambda)}\left(\frac{\alpha L}{\alpha L + 1}\right) \qquad (3)$$

where $\Phi_{ex(\lambda)}$ is the wavelength-dependent quantum yield for exciton formation[18] and α and L are the absorption coefficient and the exciton diffusion length, respectively. Thus, the maximum exciton

flux to the surface is I_oP, where I_o is the incident light intensity, and the limiting hole current density is eI_oP, where e is the electronic charge. We take the hole injection current density (into the organic layer), j_{pf}, as being a positive current and its back-reaction (and electron injection) as being negative. We assume, consistent with the usual current–overpotential equation describing heterogeneous electron transfer,[52] that the rate of carrier injection into the organic layer is an exponential function of the interfacial voltage, V_c. The expression describing a heterogeneous hole transfer current which is eventually limited (e.g., by the flux of excitons) at some limiting current, i_l, can be written (see equation 3.5.32, ref 52)

$$i = \frac{i_o i_l}{i_o + i_l e^{-(1-\alpha_p)nf\eta}} \tag{4}$$

where i_o is the exchange current, α_p is the transfer coefficient for hole injection, n is the number of holes transferred, $f = F/RT$, where F is the Faraday constant, R is the ideal gas constant, T is the absolute temperature, and η is the overpotential. In our model, n is always equal to 1.

We wish to write an equation analogous to (4) for the hole injection current density, j_{pf}, into the organic semiconductor. The limiting current density is eI_oP. We must define a quantity analogous to the exchange current (i_o in (4)) but for an irreversible photoinjection process. Thus, we define a standard rate for hole injection, j_{pf}°, as the quantum yield for hole injection under short-circuit conditions, Φ_{pf}°, times the maximum flux of excitons to the front electrode

$$j_{pf}^\circ = e\Phi_{pf}^\circ I_oP \tag{5}$$

With this definition, we can write an equation analogous to (4) for the hole injection current density, j_{pf}, into the organic layer

$$j_{pf} = \frac{ej_{pf}^\circ I_oP}{j_{pf}^\circ + eI_oPe^{-(1-\alpha_p)fV_c}} \tag{6}$$

where V_c has been substituted for η. With (5) this can be rewritten as

$$j_{pf} = eI_oP\left(\frac{\Phi_{pf}^\circ}{\Phi_{pf}^\circ + e^{-(1-\alpha_p)fV_c}}\right) \tag{7}$$

Hole Recombination, j_{pb}. At open circuit under steady-state illumination conditions, the rate of hole injection, j_{pf}, must equal the rate of hole recombination, j_{pb}. In the equivalent circuit (Figure 13), this back-reaction is modeled as a shunt resistance (R_s). Thus

$$j_{pb} = \sigma_{ps}V_c \tag{8}$$

where $\sigma_{ps} \equiv 1/AR_{ps}$ is the "rate constant" of the back-reaction in units of Ω^{-1} cm^{-2} and A is the area of the cell. Chemically this is equivalent to a first-order reaction. Thus, the recombination rate is directly proportional to the concentration of $P^{\bullet+}$ which, in turn, is directly proportional to the voltage V_c. Steady state (i.e., V_{oc}) is achieved when the (negative) voltage reaches a value such that the linearly increasing rate of the back-reaction is equal and opposite to the exponentially decreasing rate of the forward reaction.

Hole Current, j_{po}. When the circuit is closed, the total hole current is equal to the difference between the rate of injection and the rate of recombination. Thus, from (7) and (8)

$$j_{po} = eI_oP\left(\frac{\Phi_{pf}^\circ}{\Phi_{pf}^\circ + e^{-(1-\alpha_p)fV_c}}\right) + \sigma_{ps}V_c \tag{9}$$

Single Carrier Photovoltage, V_{oc}. The open-circuit photovoltage can be calculated from (9) by setting the current equal to zero and rearranging. However, because of the nonlinear term, an explicit expression for V_{oc} as a function of I_o cannot be written. I_o is therefore expressed as a function of V_{oc}:

$$I_o = \frac{-\sigma_{ps}V_{oc}}{eP}\left\{1 + \frac{e^{-(1-\alpha_p)fV_{oc}}}{\Phi_{pf}^\circ}\right\} \tag{10}$$

A plot of (10) is shown in Figure 14a.

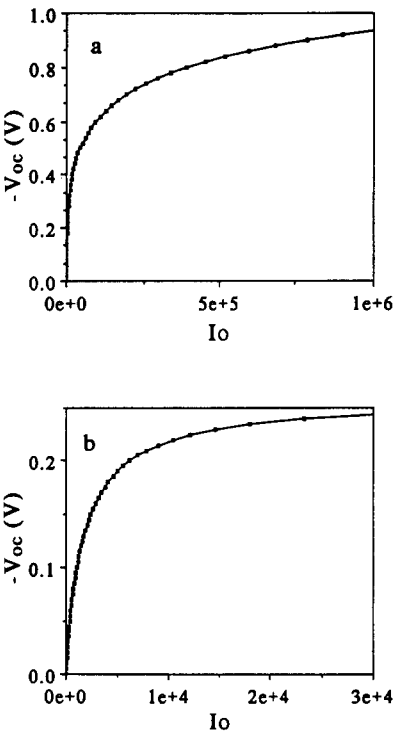

Figure 14. Calculated photovoltage vs intensity curves for the case of (a) only hole injection, from (10), and (b) both hole and electron injection, from (14). In both cases $\Phi_{pf}^\circ = 0.05$, $\sigma_{ps} = 47\ \Omega^{-1}$ cm^{-2}, $\alpha_p = 0.85$, $P = 0.2$, and I_o is in units of 10^{12} photons s^{-1} cm^{-2}. In (b) $\Phi_{nf}^\circ = 0.0025$, $\alpha_n = 0.15$.

Electron Injection. The equations describing a cell in which only electron injection (into the organic layer) takes place can be derived in a manner analogous to those for hole injection. Thus, the equation for the electron injection current density corresponding to (9) is

$$j_{no} = -eI_oP\left(\frac{\Phi_{nf}^\circ}{\Phi_{nf}^\circ + e^{\alpha_n fV_c}}\right) + \sigma_{ns}V_c \tag{11}$$

Both Hole and Electron Injection. In some systems (Figure 12B), both electrons and holes can be injected into the organic layer depending on the voltage. At low voltages, e.g., in the power-curve region, both carriers can be injected simultaneously. In this case we assume that the carriers recombine in the bulk leaving an excess of only one type of carrier (the majority carrier). Thus we consider that the total current, j_o, is equal to the sum of the (positive) hole current and the (negative) electron current:

$$j_o = j_{po} + j_{no} \tag{12}$$

Dual Carrier Photovoltage. The open-circuit photovoltage in the case of both electron and hole injection can be derived by setting (12) to zero and substituting (9) and (11) into the result:

$$eI_oP\left(\frac{\Phi_{pf}^\circ}{\Phi_{pf}^\circ + e^{-(1-\alpha_p)fV_{oc}}}\right) + \sigma_{ps}V_{oc} = eI_oP\left(\frac{\Phi_{nf}^\circ}{\Phi_{nf}^\circ + e^{\alpha_n fV_{oc}}}\right) - \sigma_{ns}V_{oc} \tag{13}$$

Only one back-reaction is operative at any voltage; by assumption, the injected minority carriers recombine in the bulk with the majority carriers. Thus, if V_{oc} is negative (i.e., holes are being

(52) Bard, A. J.; Faulkner, L. R. *Electrochemical Methods*; Wiley: New York, 1980.

preferentially injected into the LCP), the recombination reaction of electrons at the electrode can be neglected. Equation 13 can then be rearranged to

$$I_o = \frac{-\sigma_{ps} V_{oc}}{eP}\left\{\left(\frac{\Phi_{pf}^\circ}{\Phi_{pf}^\circ + e^{-(1-\alpha_p)fV_{oc}}}\right) - \left(\frac{\Phi_{nf}^\circ}{\Phi_{nf}^\circ + e^{\alpha_n fV_{oc}}}\right)\right\}^{-1} \quad (14)$$

Again, V_{oc} cannot be expressed as an explicit function of I_o. A plot of (14) is shown in Figure 14b. In the case of both electron and hole injection, in contrast to the single carrier injection case, V_{oc} does saturate with I_o. The maximum V_{oc} occurs when

$$\left(\frac{\Phi_{pf}^\circ}{\Phi_{pf}^\circ + e^{-(1-\alpha_p)fV_{oc,max}}}\right) = \left(\frac{\Phi_{nf}^\circ}{\Phi_{nf}^\circ + e^{\alpha_n fV_{oc,max}}}\right) \quad (15)$$

or

$$V_{oc,max} = \frac{kT}{e(\alpha_p - \alpha_n - 1)} \ln\left(\frac{\Phi_{pf}^\circ}{\Phi_{nf}^\circ}\right) \quad (16)$$

More Realistic Model: Inclusion of Resistance-Limited Currents and Bulk Carrier Generation. The model described above is valid for open-circuit conditions ($i = 0$, i.e., when $V = V_c$) as well as for those cases when the cell resistance is so low that the current is limited only by the exciton flux to the interface. In many circumstances, however, the current will be limited by the resistance of the cell. This leads to a substantial increase in the complexity of the model. This case could be treated, for example, by a numerical solution of an equation similar to (9) but including the effect of the bulk resistance, e.g., with the substitution $V_c = V + iR = V + AjR$:

$$j_p = eI_o P\left(\frac{\Phi_{pf}^\circ}{\Phi_{pf}^\circ + e^{-(1-\alpha_p)f(V+Aj_pR)}}\right) + \sigma_{ps}(V + Aj_pR) \quad (17)$$

In the present work, however, there is the added complication that R is a function of both light intensity and wavelength; i.e., photoconductivity effects are important. To demonstrate that our experimental results, most notably the action spectra, can be explained by a simple consideration of the bulk photoconductivity of the LCP cells, we use a linear approximation to (17) based on the following considerations. At low current densities, the iR term can be neglected, thus $V_c \approx V$. As the current density increases, the fraction of the measured voltage (V) that drops across the illuminated interface (V_c) decreases, while the fraction of V that drops across the bulk (iR) increases. Eventually, the current is almost entirely controlled by the bulk resistance leading to a linear increase of i with V (see, for example, Figure 7). Therefore, the current should at first be an exponential function of the voltage and eventually be limited by the resistance of the cell. Thus, we make the following approximations: (1) $V_c = V$; (2) the limiting current (i.e., i_l in (4)) is a function of the cell resistance; and (3) the current density is resistance-limited only above a certain threshold given by $j_l = V_o/R$, where R is the total cell resistance and V_o is an adjustable parameter.

The bulk resistance, R, has two components: one due to the injected carriers and one due to the carriers photogenerated in the bulk. We have used the following approximate equation (derived in the Appendix) to describe the resistance-limited current for hole injection:

$$j_{pl} = eI_o\mu_p\left\{\frac{Pt_g}{d^2} + \frac{t_b}{\Phi_{ex(\lambda)}}\left(\frac{\alpha^2}{e^{\alpha d/a} - 1}\right)\right\}(|V - V_{oc}| + V_o) \quad (18)$$

where μ_p is the hole mobility; d is the cell thickness; t_g and t_b determine the relative contributions of the injected and bulk generated carriers, respectively, to the total photocurrent; and a is an approximate correction factor that is taken equal to 2. The resistance-limited current for electron injection, j_{nl}, is analogous to (18) with the substitution of the electron mobility for that of holes.

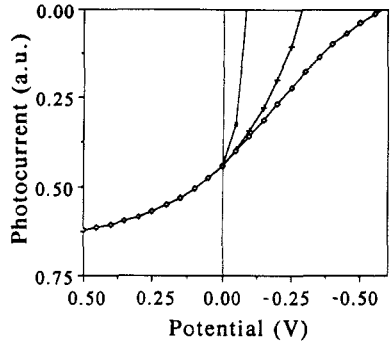

Figure 15. Calculated photocurrent–voltage curves for the case of hole injection only. Calculated from (20) with $\Phi_{pf}^\circ = 0.05$ and the back-reaction parameter (Ω^{-1} cm^{-2}), $\sigma_{ps} = 100$ (solid squares), 10 (crosses), and 1 (open diamonds).

Back-Reaction. The expression describing the rate of the back-reaction of holes at the illuminated electrode, (8), is valid only between the limits $V_{oc} \le V (= V_c) \le 0$, i.e., in the power-curve region. The lower limit (V_{oc}) stems from the fact that the rate of the back-reaction cannot exceed the rate of the forward reaction at steady state (holes cannot recombine faster than they are generated). The upper limit stems from our assumptions that $V = V_c$ and that only holes are being photoinjected; thus V_c, and therefore j_{pb}, must always be negative. Because of the limited zone of applicable voltages for (8), it is convenient to make a continuous approximation to it that can be used to calculate approximate current–voltage curves over the whole range of V. Thus, we write

$$j_{pb} \approx \frac{\sigma_{ps} V N j_{pf}}{\sigma_{ps} V + N j_{pf}} \quad (19)$$

where $N > 1$. This equation means that the rate of the back-reaction is limited at some multiple (N) of the rate of the forward reaction. In practice, the rate of the back-reaction can never exceed the rate of the forward reaction (i.e., $N = 1$); however, since j_{pf} is decreasing exponentially as V becomes more negative, the error caused by the use of (19) rather than (8) can be small. Equation 19 can be used for $V \le 0$, and the corresponding equation for electron recombination can be used for $V \ge 0$.

Both Hole and Electron Injection, Resistance Limited. A final expression for the current–voltage characteristics under resistance-limited conditions can now be given. The total current, j, is equal to the sum of the hole current and the electron current, the total being limited by the resistance-limited current for whichever carrier is in excess

$$j = \frac{(j_{po} + j_{no})j_l}{|j_{po} + j_{no}| + j_l} \quad (20)$$

where $j_l = j_{pl}$ when excess holes are being injected and $j_l = j_{nl}$ when excess electrons are being injected.

In the limit when only one carrier is injected, the term for the opposite carrier in (20) is zero. Thus, when only holes are injected, $j_{no} = 0$ and $j_l = j_{pl}$. Furthermore, in this case, the more exact expression for the recombination, (8), can be used. Figure 15 shows several plots of (20) for different values of the recombination "rate constant" σ_{ps} when only holes are injected. The curves diverge exactly at $V = 0$ because of the assumption that $V = V_c$; thus there is no back-reaction for $V > 0$. Similar photocurrent–voltage curves have been observed in thin films of phthalocyanine[44] and tetracene.[53]

For the case of dual-carrier injection, several plots of (20) versus voltage are shown in Figure 16 for different values of the standard quantum yield for electron injection, Φ_{nf}°. The change in the current–voltage curves, calculated from (20), with a change in the amount of bulk generated carriers (t_b), i.e., with a change in

(53) Lyons, L. E.; Newman, O. M. G. *Aust. J. Chem.* **1971**, *24*, 13.

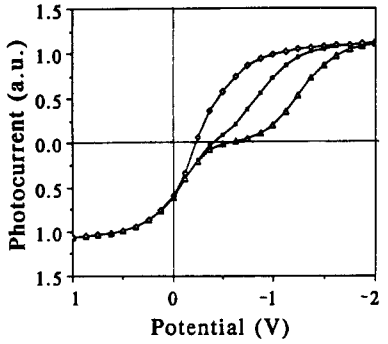

Figure 16. Calculated photocurrent–voltage curves for the case of both hole and electron injection. Calculated from (20) and (19) with $N = 5$, $t_b = 10^{-4}$ s, $\Phi_{pf}^{\circ} = 0.05$, $\sigma_{ps} = \sigma_{ns} = 47\ \Omega^{-1}\ cm^{-2}$, $\mu_p = \mu_n = 1\ cm^2\ V^{-1}\ s^{-1}$ and with $\Phi_{nf}^{\circ} = 2.5 \times 10^{-3}$ (diamonds), 2.5×10^{-4} (squares), and 2.5×10^{-5} (triangles). Cathodic currents are plotted up.

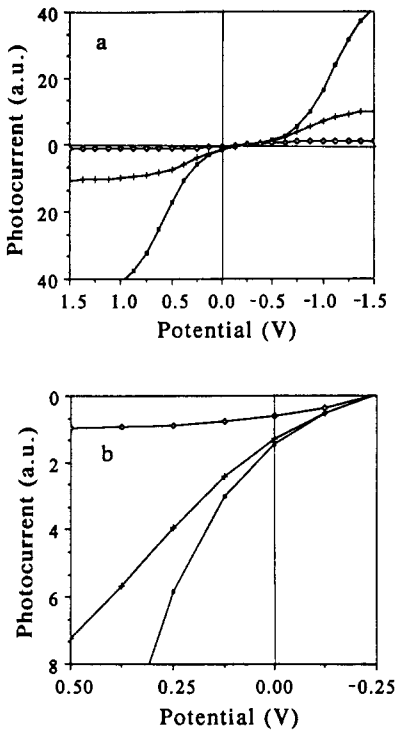

Figure 17. Calculated photocurrent–voltage curves for the case of both hole and electron injection for different rates of bulk carrier generation (proportional to t_b), i.e., different values of the bulk resistance. Calculated from (20) and (19) with $N = 5$, $\Phi_{pf}^{\circ} = 0.05$, $\Phi_{nf}^{\circ} = 2.5 \times 10^{-3}$, $\sigma_{ps} = \sigma_{ns} = 47\ \Omega^{-1}\ cm^{-2}$, $\mu_p = \mu_n = 1\ cm^2\ V^{-1}\ s^{-1}$ and with $t_b(s) = 10^{-4}$ (diamonds), 10^{-3} (crosses), and 5×10^{-3} (solid squares). (b) An enlarged view of the power-curve region of (a). Cathodic currents are plotted up.

the level of the bulk resistance, is shown in Figure 17. The calculations shown in Figures 16 and 17 employed (19) with $N = 5$.

Equation 20 can also be used to calculate the wavelength dependence of the photocurrent (action spectra). The change in the calculated short-circuit action spectra with cell thickness is shown in Figure 18.

Evaluation of the Model and Comparison with Experiment

The results presented here are consistent with two mechanisms of charge carrier production, bulk generation, and photoinjection, operating in concert. We believe that it is not possible to rationalize our results with either mechanism alone. We first discuss bulk generation.

Bulk Generation. It has been suggested[43] that if illumination results in the production of one free carrier and the trapping of the opposite carrier, a photovoltaic effect can result from the increase in the number of free carriers near the illuminated electrode. However, Landau and Lifshitz[43] have shown that, as

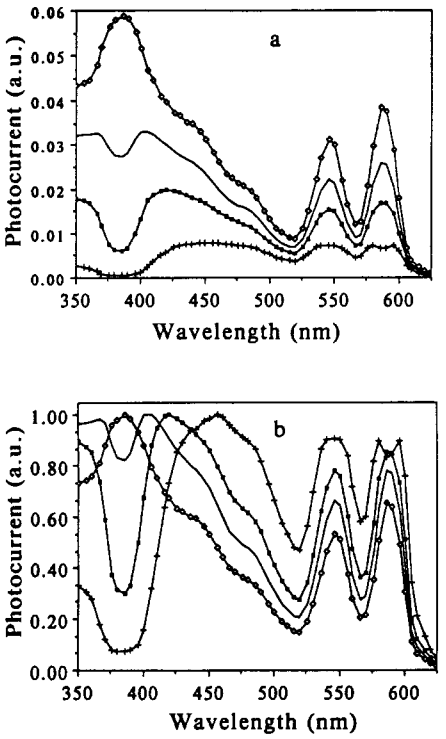

Figure 18. Calculated action spectra at various cell thicknesses from (20). See text for parameters used. The spectra were calculated for d (μm) = 1 (diamonds), 2 (solid), 3 (squares), and 5 (crosses). (a) Action spectra as calculated. (b) Normalized action spectra.

long as the carriers have a Maxwellian velocity distribution, a photovoltaic effect cannot result from this mechanism. Another possible explanation of the photovoltaic effect is that equal and opposite space charge layers are formed at both ITO–porphyrin interfaces, the photovoltaic effect being determined at the illuminated interface. The formation of two space charge layers in a 2-μm-thick cell, however, would require a doping density of ca. 10^{14} cm^{-3} or greater.[29,32,39] This is unlikely given the previous discussion and the fact that the dark current was too low to measure. In single-crystal phthalocyanine, for example, the carrier density has been measured as 10^5–10^7 cm^{-3}.[26c] Furthermore, if a space charge layer formed (i.e., if the porphyrin attained equilibrium with its electrodes), the open-circuit photovoltage should be a function of the redox potential of the porphyrin and of the concentration of added dopant (e.g., DDQ); this was not observed.

The Dember effect[29] can be ruled out on the basis of the lack of a substantial change in the photocurrent action spectrum upon voltage reversal (Figure 9) and by the small difference in the limiting currents under positive and negative bias (Figures 7 and 10) which implies only a small difference in electron and hole mobility; see below. *Thus, we believe that the photovoltaic effect in these LC porphyrin cells cannot be caused by the bulk generation of charge carriers.*

Photoinjection. A number of the results discussed above led us to expect that the photoinjection of carriers into the porphyrin layer should play some role in these devices. If one carrier is photoinjected preferentially over the other at zero applied bias, this process must lead to a photovoltage and, under short-circuit conditions, to a photocurrent. Photoinjection at a surface has been widely regarded as the predominant carrier generation process in cells containing polycyclic aromatic hydrocarbons (PAHs).[24,26a,c,d] However, devices involving porphyrins and phthalocyanines have commonly been discussed in the same terms as inorganic semiconductor devices;[3-13,26b] i.e., space charge layers and bulk generation of carriers have been assumed. One possible explanation for this discrepancy is that it is relatively easy to make devices from highly purified, single crystals of PAHs, while the porphyrins and phthalocyanines are more difficult to purify and crystallize as needles rather than as plates.[23] Thus, the devices

employing the latter compounds are usually in the form of evaporated amorphous or microcrystalline layers having a much larger effective surface area (which can promote exciton dissociation) than a single crystal of the same geometric area. Moreover, the grain boundaries between crystallites are known to concentrate impurities which can lead to carrier formation either directly or though trap-mediated exciton dissociation.[24,26,29] Thus, one would expect an amorphous or microcrystalline layer to exhibit a higher carrier density (and a lower carrier mobility) than a single crystal of the same material. This higher carrier density may allow junction formation in a manner similar to inorganic semiconductors.

Perhaps the greatest difference between the liquid crystalline porphyrins described here and previously studied porphyrins and phthalocyanines is the tendency of the LCPs to form large crystallites. Almost all of the crystallites in the LCP cells were substantially larger in diameter than the cell thickness and spanned the cell (see, for example, Figure 4, ref 17). (The cells containing H_2OOEP were exceptional; they contained microscopic crystallites and had much smaller photocurrents than the metallo derivatives.) Thus, the devices containing metallo-LCPs are more closely related to single-crystal cells than they are to cells made from evaporated films. *It seems that the predominance of carrier photoinjection over bulk generation in some organic solar cells may be more a function of crystallinity and purity than of the chemical identity of the compound (e.g., PAHs vs porphyrins and phthalocyanines).*

Another interesting facet of the LC porphyrins is that the chromophores are surrounded by an insulating hydrocarbon layer. Thus, the conductivity is much more one-dimensional in the LCP than in the conventional porphyrins and phthalocyanines. This places additional importance on the crystallinity of the LCP films: since ca. two-thirds of the volume taken up by an LCP molecule consists of insulating hydrocarbon, an amorphous LCP layer would be expected to be a very poor electronic conductor.

An organic solar cell based on photoinjection might have some advantages over a conventional one based on bulk carrier generation. For example: the diffusion length of an exciton is often much longer than that of a bulk generated carrier;[24,26] thus, excitons can be collected from a larger fraction of the cell volume than can bulk carriers. Furthermore, if only one carrier is photoinjected, recombination can occur only at the electrodes since the bulk contains only one type of carrier.

Photovoltage vs Intensity. Bonham[45] and Pope and Swenberg[26a] derived an expression for the photovoltage resulting from a single carrier photoinjection process:

$$V_{oc} = \frac{kT}{e} \ln\left(\frac{1 + aI_o}{1 + bI_o}\right) \qquad (21)$$

where a is the ratio of carrier injection rates in the light and the dark at the front electrode, b is the corresponding quantity, times an attenuation factor for the light intensity, at the back electrode, and I_o is the incident light intensity. This equation is based on a calculation of the change in the quasi-Fermi level with carrier concentration. Thus, it predicts that V_{oc} should increase with the logarithm of the ratio of the carrier concentrations at the front and back electrodes. However, we believe that this expression does not adequately account for the charge on the carriers. The injection process results in an electrostatic charging of the two phases (the organic phase and the electrode). The injected carrier density is *equal* to the charge density which, by Gauss's law, should be linearly proportional to the voltage difference between the two phases. Hence, V_{oc} should increase linearly with the bulk carrier concentration.

Thus, although behavior similar to that predicted by (21) has often been observed,[26a,42,44,45] we believe that a better expression is given by (10) for the single-carrier case and by (14) for the case of dual-carrier injection. We note that (14) predicts the same form of the V_{oc} dependence on intensity as does (21). Furthermore, if (10) were modified to include the effect of excitons reaching the back surface, it would then be of approximately the same form as (14) and would also predict the eventual saturation of V_{oc} with intensity. Thus our model is compatible with the previously reported behavior.[26a,42,44,45]

The photovoltage of the LCP cells increased almost linearly with incident intensity (I_o) at low intensity and eventually saturated at higher I_o (Figure 3). Given the fact that these cells exhibit both electron and hole injection (see Figures 7 and 10), we fit our data to (14). We initially assumed that $\alpha_p + \alpha_n = 1$; this turned out to give a good fit to the data. The maximum V_{oc} reached by the cell in Figure 3 was −0.26 V. Insertion of this value into (16) gave a series of values for the ratio $(\Phi_{pf}^\circ/\Phi_{nf}^\circ)$ and their associated values of $(\alpha_p - \alpha_n - 1)$. These were inserted into (14) along with an assumed value of $P = 0.2$ (this requires $L = 0.25$ μm and $\Phi_{ex(\lambda)} = 1$ at $\lambda = 585$ nm[18]), and the results were plotted for various values of σ_{ps}. The best fit obtained is shown in Figure 3 and employed the following values: $\Phi_{pf}^\circ = 0.05$, $\Phi_{nf}^\circ = 0.0025$, $\sigma_{ps} = 47\ \Omega^{-1}\ cm^{-2}$, $\alpha_p = 0.85$, and $\alpha_n = 0.15$. These values were used in the remaining calculations. This procedure cannot give an absolute value of Φ_{pf}° or Φ_{nf}° but only their ratio. We simply chose $\Phi_{pf}^\circ = 0.05$ as being a reasonable value. The ratio of $(\Phi_{pf}^\circ/\Phi_{nf}^\circ)$ suggests that, when $V_c = 0$ (e.g., at short circuit, under low light intensity), *hole injection into the LCP is approximately 20 times more likely than electron injection.* The values of the transfer coefficients, α_p and α_n, determine the shape of the photovoltage vs intensity curve and are probably accurate to ±0.03.

The value of L assumed above ($L = 0.25$ μm) is in the normal range of exciton diffusion lengths for organic crystals.[26,40] We were not able to calculate L in the usual fashion[26,40] from the action spectra because of the interaction between the injection and the bulk currents. Our results would not be greatly affected by a change in L of ±25%.

Photovoltage vs Wavelength. The two theoretical curves in Figure 4 were calculated using the theoretical curve of Figure 3 and the fact that a variation in P with wavelength is equivalent to a variation in I_o at constant P (see (14)). The upper curve is calculated assuming a quantum yield for exciton formation, $\Phi_{ex(\lambda)} = 1$ for all wavelengths. The lower curve uses the values of $\Phi_{ex(\lambda)}$ measured in ref 18 which decrease with increasing energy of excitation. The fit is much better when the measured $\Phi_{ex(\lambda)}$ is used, although it is not perfect. The photovoltage spectra were quite reproducible but did not correspond exactly to the absorption spectra.

Short-Circuit Photocurrent. The short-circuit current of these cells increased linearly with incident intensity over a large range of intensities (Figure 5a). This rules out any two-photon mechanisms for the production of charge carriers. It also indicates that space charge effects and carrier recombination are unimportant in this intensity range.[23,26a,c,54,55] *These data allow a calculation of Φ_{sc}, the short-circuit quantum efficiency for current production: at $\lambda = 400$ nm, this cell exhibited a $\Phi_{sc} \approx 2\%$.* At higher intensities (Figure 5b), the short-circuit current increased with the square root of the intensity. The short-circuit current was surprisingly stable, decreasing by ca. 15% over the first 30 min of illumination and then remaining constant over several days. This corresponds to the passage of ca. 10^4 electrons per porphyrin molecule, thus demonstrating the chemical stability of the porphyrins in this system.

Single vs Dual Carrier Injection. For systems in which only one carrier is injected, the open-circuit photovoltage and the shape of the power curve are entirely determined by the relative rates of the forward and back reactions (see (10) and (20) and Figure 15). Since the back-reaction rate is a function only of the voltage, V_c, (i.e., the number of injected carriers), an increase in the forward reaction rate (e.g., by an increase in the light intensity) must always lead to an increase in the photovoltage to maintain the steady state. Thus the photovoltage does not saturate with intensity (Figure 14a). However, as noted above, if the effect of excitons reaching the unilluminated electrode were taken into account, the photovoltage in the single-carrier case would eventually saturate with intensity.

(54) Lyons, L. E.; Mackie, J. C. *J. Chem. Soc.* **1960**, 5186.
(55) Kommandeur, J.; Schneider, W. G. *J. Chem. Phys.* **1958**, *28*, 582.

For systems in which both carriers can be injected, V_{oc} and the power curve are determined by the competition between the injection rates of both carriers and the back-reaction rate of majority carriers (see (14) and (20) and Figure 16). Since the recombination rate of majority carriers is dependent both on the photovoltage and on the injection rate of minority carriers, the photovoltage does saturate with intensity. The maximum photovoltage that can be reached (16) is the voltage at which the minority carrier injection rate exactly equals the majority carrier injection rate. The rate at which this maximum is approached with increasing intensity depends on the rate constant of the back-reaction (σ_s).

Resistance Effects on the i–V Curves. The undoped LCP cells all showed a characteristic S-shaped i–V curve (Figures 7 and 10) similar to the curve calculated in Figure 16 with $\Phi_{pf}^{\circ} = 0.05$, $\Phi_{nf}^{\circ} = 0.0025$, $V_o = 10$ V, $t_g = 3 \times 10^{-5}$ s, $t_b = 1 \times 10^{-4}$ s, and $\mu_p = \mu_n = 1$ cm^2 V^{-1} s^{-1}. Figure 17 shows the calculated effect of increasing only the bulk conductivity (i.e., increasing t_b in (18)) on the i–V curves. The curves exhibit a flattened appearance around zero and increase sharply at higher voltage. This is the same effect observed in solution-phase electrochemistry when the limiting current is increased relative to the exchange current.[52] Such a change in shape of the i–V curves is seen in DDQ-doped cells (Figure 11) which show a large increase in the limiting current relative to that of undoped cells.

Figure 17b shows the power-curve region of the i–V curves shown in Figure 17a. The photovoltage is unaffected by the change in conductivity but the short-circuit photocurrent is increased. In the DDQ-doped cells, neither V_{oc} nor i_{sc} changed substantially from the undoped case. This can be explained by noting that the increase in (exciton-mediated) bulk carrier generation causes a decrease in the number of excitons reaching the front surface; thus, the increase in the bulk conductivity is offset by a decrease in the injection current. This would not affect the maximum V_{oc} of the cell (see above and (16)) but should require a higher light intensity to reach the maximum V_{oc} than in an undoped cell. This interaction between the numbers of bulk generated carriers and injected carriers is not contained in the model, where it is assumed that the two processes are independent.

Relative Carrier Mobilities. The limiting photocurrent under a negative applied bias was always 2–3 times higher than under a positive bias (Figures 7 and 10). In other words, $j_{nl} \geq 2j_{pl}$ (18). This is most easily explained by assuming that *the electron mobility is higher than that of holes, i.e., $\mu_n \geq 2\mu_p$, in the LCP.*

Action Spectra. Action spectra in which the current peaks do not match the absorption peaks have been observed previously. This can result from carrier recombination,[55] space charge effects,[23,54] or an optical filtering effect.[3d,g] As mentioned, the data of Figure 5a indicate that recombination is unimportant under the illumination conditions of our action spectra. These same data are also incompatible with the existence of space charge limitations to the current which would be expected to cause a sublinear increase of i_{sc} with I_o.[23] Furthermore, the action spectra would be expected to change substantially with applied voltage for any of the above-mentioned effects. In our case, however, the action spectra change only slightly with voltage (Figure 9).

To our knowledge, a change in action spectra with thickness, such as observed in the LCP cells (Figure 8), has not been previously reported. As explained above, we interpret this effect as resulting from the interaction between the bulk photoconductivity and the injection current.[56] For thick cells, weakly absorbed light will penetrate deeply into the sample, reducing the resistance and increasing the current at these wavelengths compared to the current at more strongly absorbed wavelengths where the resistivity of much of the cell is practically at its dark level (see (18)). Thus, for thick cells, the photocurrent action spectrum will show minima at the peaks of the absorption spectrum. As the cell thickness is decreased, the strongly absorbed light will penetrate a substantial portion of the sample, while only a fraction of the weakly absorbed light will be absorbed by the cell. At this point the spectral characteristics of the bulk and injected currents should be similar (neglecting the effect of $\Phi_{ex(\lambda)}$). Thus, for thin cells, the action spectra will be correlated with the absorption spectra. These effects are also observed in the j–V curves (Figure 10). One consequence is that the wavelength at which the cell shows its maximum quantum efficiency is a function of the cell thickness.

Equation 20 was used to calculate a set of action spectra vs cell thickness (Figure 18a,b). Our purpose was not to attempt a quantitative fit to the data, but rather to show that the model can qualitatively reproduce the essential features. The values of the injection current parameters in these calculations were the same as those used in the V_{oc} vs I_o calculation. The parameters governing the resistance were set as follows: μ_p and ϵ were taken to be 1, $a = 2$, $V = 0$ V, $V_o = 30$ V, $t_g = 3 \times 10^{-5}$ s, and $t_b = 1 \times 10^{-4}$ s. The variables used in (20) for the calculations were, at 5-nm intervals, the absorption coefficient, α, the quantum yield for exciton formation, $\Phi_{ex(\lambda)}$, and the V_{oc} data calculated above.

The calculated action spectra (Figure 18) agree qualitatively with the experimental spectra (Figure 8), although (20) underestimates the current in the Soret band region in the thicker cells. If t_b was taken as = 0, i.e., *under conditions where no bulk generation of carriers takes place, the calculated photocurrents were greatly reduced and the wavelength dependence of the photocurrent was independent of thickness and always resembled the absorption spectrum.* This corresponds to the pure photoinjection case.

Summary

A novel photovoltaic effect in symmetrical cells containing a liquid crystal porphyrin has been described and explained on the basis of preferential hole photoinjection into the LCP at the illuminated interface. Our analysis suggests that hole injection is approximately 20 times more likely than electron injection under conditions of zero interfacial voltage. This appears to be the first example of a photovoltaic cell that is entirely controlled by interfacial kinetics rather than by a gradient of electrochemical potential. The predominance of the photoinjection process in these cells, and its relative absence in evaporated porphyrin and phthalocyanine films, led to the suggestion that the magnitude of the photoinjection process is more characteristic of the purity and crystallinity of the organic material than of its chemical identity. The magnitude of the photocurrent and its unusual dependence on wavelength and cell thickness led to the conclusion that photogenerated bulk carriers contribute to a wavelength-dependent photoconductivity. An approximate mathematical model of the photovoltaic behavior, based on an equivalent circuit description, was developed and shown to reproduce the essential features of the data. Our results show that a substantial photovoltaic effect can be realized without the requirement for a space charge layer. Further investigation into the mechanism of the asymmetric dissociation of excitons at the molecular semiconductor/electrode interface may lead to a new design for organic solar cells.

Acknowledgment. We are grateful to the National Science Foundation for support of the Materials Research Group at the University of Texas, under whose aegis this work was performed.

Appendix. Approximation of the Resistance-Limited Current

The resistance-limited hole current should have two components: one due to the injected holes and one due to the bulk generated carriers (we neglect the effect of the dark carriers). We will assume that the limiting current density due to injected holes, j_{pgl}, has the usual form for an ohmic (non-space-charge-limited) current in a photoconductor:[57]

$$j_{pgl} = eI_oP\mu_p\tau_p(V - V_{oc})/d^2 \qquad \text{(A1)}$$

(56) A related effect has been studied by Gerischer et al. in inorganic insulators. In these cases, illumination by strongly absorbed light led to very low photocurrents. Additional illumination by a second, weakly absorbed light led to a large increase in quantum efficiency. This was explained as being caused by an increase in bulk photoconductivity due to the weakly absorbed light. See: (a) Gerischer, H.; Lübke, M.; Bressel, B. *J. Electrochem. Soc.* **1983**, *130*, 2112. (b) von Känel, H.; Kaldis, E.; Wachter, P.; Gerischer, H. *J. Electrochem. Soc.* **1984**, *131*, 77.

where e is the electronic charge, I_0P is the maximum hole injection rate, μ_p is the mobility of the hole, τ_p is its lifetime, d is the cell thickness, and $V - V_{oc}$ is the effective voltage on the cell.

The second component of the bulk resistance is assumed to be proportional to the number and spatial distribution of the photogenerated carriers. We assume that the resistivity, $\rho(x)$, of an infinitesimal slab of thickness dx is inversely proportional to the number of charge carriers in the slab. The total resistance, R, of the cell due to bulk generated carriers is then given by[32]

$$R = \int_0^d \rho(x)\,dx = \int_0^d \frac{1}{e\mu_0 n_t(x)}\,dx \qquad (A2)$$

where $n_t(x)$ is the concentration of bulk generated carriers (electrons and holes) and μ_0 is an average mobility of the carriers. $n_t(x)$ can be calculated from a continuity equation[32] with neglect of diffusion and recombination:

$$n_t(x) = I_0\Phi_{b(\lambda)}\tau_0\alpha e^{-\alpha x} \qquad (A3)$$

where $\Phi_{b(\lambda)}$ is the wavelength-dependent quantum yield for formation of carriers in the bulk, α is the absorption coefficient, τ_0 is the average lifetime of the carriers, and x is the distance inside the sample measured from the illuminated electrode. Insertion of (A3) into (A2) and integration leads to

$$R = \frac{1}{e\mu_0\tau_0 I_0\Phi_{b(\lambda)}}\left(\frac{e^{\alpha d}-1}{\alpha^2}\right) \qquad (A4)$$

(57) Rose, A. *Concepts in Photoconductivity and Allied Problems*; Interscience: New York; 1963.

Equation A4 must overestimate the cell resistance, since it neglects the effect of both carrier drift and diffusion and it neglects the effect of exciton diffusion before dissociation into charge carriers. This can be partially offset through the introduction of an adjustable parameter, a, into the exponential term; in our calculations we have taken $a = 2$. The inverse of R, modified by a and multiplied by the effective cell voltage $(V - V_{oc})$, gives the ohmic current, j_b, resulting from the bulk carriers

$$j_b = eI_0\mu_0\tau_0\Phi_{b(\lambda)}\left(\frac{\alpha^2}{e^{\alpha d/a}-1}\right)(V - V_{oc}) \qquad (A5)$$

We assume that the mobility in (A5) can be taken as equal to the mobility of holes, μ_p, since the bulk carriers are predominantly created near the illuminated electrode and, under conditions of hole injection, the holes must migrate further than the electrons.

Combining (A1) and (A5) leads to an approximate expression for the resistance-limited hole current

$$j_{pl} = eI_0\mu_p\left\{\frac{Pt_g}{d^2} + \frac{t_b}{\Phi_{ex(\lambda)}}\left(\frac{\alpha^2}{e^{\alpha d/a}-1}\right)\right\}(|V - V_{oc}| + V_0) \qquad (18)$$

where t_g is a characteristic time for the injection process which includes τ_p and determines the relative contribution of the injected carriers to j_{pl}. t_b is the corresponding quantity for bulk generated carriers. $\Phi_{b(\lambda)}$ is assumed to be proportional to $1/\Phi_{ex(\lambda)}$,[40] with the proportionality constant included in t_b. The absolute value of $V - V_{oc}$ has been used as a convenience to ensure that j_{pl} is a positive quantity. V_0 determines the minimum value of the current above which the current is assumed to be resistance limited. That is, the current will be resistance limited when it is above the value $i = V_0/R$, where R is the total resistance of the cell.

Synthesis of Cadmium Sulfide in Situ in Reverse Micelles. 2. Influence of the Interface on the Growth of the Particles

C. Petit,† P. Lixon,‡ and M. P. Pileni*,†,‡

Université P. et M. Curie, Laboratoire S.R.I. bâtiment de Chimie Physique, 11 rue P. et M. Curie 75005 Paris, France, and C.E.N. Saclay, D.L.P.C.-S.C.M Bât. 522, 91191 Gif sur Yvette, France *(Received: June 12, 1989)*

AOT reverse micelles make possible the in situ synthesis of very small particles of CdS. The use of functional surfactants (such as cadmium lauryl sulfate or cadmium AOT) allows, by blocking one of the reactants at the interface of the micelles, semiconductor colloids to be obtained that are more stable and smaller than those obtained from ions solubilized in the water pool of the reverse micelle. A comparative study of the different conditions of synthesis is presented to optimize the production of very small aggregates without having to use a protecting agent. The behavior of these semiconductors with respect to photocorrosion is studied.

Introduction

The use of dispersed media to solubilize or synthesize microparticles in situ has made considerable progress in the past few years: Langmuir–Blodget films,[1] vesicles,[2] polymerized vesicles,[3] double layers,[4] or reverse micelles[5-9,13] have been used as the incorporation media for microparticles, colloids, or semiconductors. Particles such as CdS or TiO_2 are preferred materials for these studies as they can bring about photochemical reactions when they are irradiated with visible light or near-UV light.[10] In some cases the modifications in the structure of the electron bands due to the very small size of the particles allow one to obtain reactions that are impossible with bulk material.[11] Cadmium sulfide has been synthesized in AOT reverse micelles,[5-9] with very high concentrations of surfactant (AOT = 0.5 M) and in the presence of small quantities of water. These authors[5,7-9] were able to observe

* To whom correspondence should be addressed.
† Université P. et M. Curie.
‡ C.E.N. Saclay.

(1) Asaolu, I. A.; Blott, B. H.; Khan, W. I.; Melville, D. *Thin Solid Films* **1983**, *99*, 263.
(2) (a) Tricot, Y. M.; Fendler, J. H. *J. Phys. Chem.* **1986**, *90*, 3669. (b) Watzke, H. J.; Fendler, J. H. *J. Phys. Chem.* **1985**, *89*, 854.
(3) Tricot, Y. M.; Emeren, A.; Fendler, J. H. *J. Phys. Chem.* **1986**, *89*, 565.
(4) Mann, S.; Hannington, S. P.; Williams, R. J. P. *Nature* **1986**, *324*, 565.
(5) Meyer, M.; Wallberg, C.; Kurihara, K.; Fendler, J. H. *J. Chem. Soc., Chem. Comm.* **1984**, *90*, 90.
(6) Petit, C.; Pileni, M. P. *J. Phys. Chem.* **1988**, *92*, 2282.
(7) (a) Lianos, P.; Thomas, J. K. *Chem. Phys Lett.* **1986**, *125*, 299. (b) Lianos, P.; Thomas, J. K *J. Colloid Interface Sci.* **1987**, *117*, 505.
(8) Dannhauser, T.; O'neal, M.; Johansson, K.; Whitten, D.; McLennon, G. *J. Phys. Chem.* **1986**, *90*, 6074.
(9) Steigewald, M. L.; Alirisatos, A. P.; Gibson, J. M.; Harris, T. D.; Korten, R.; Muller, A. J.; Thoyer, A. M.; Duncan, T. M.; Douglas, D. C.; Brus, L. E. *J. Am. Chem. Soc.* **1988**, *110*, 3046.

0022-3654/90/2094-1598$02.50/0